Progress In Electromagnetics Research, PIER 82, 433–445, 2008

AN EQUIVALENT CIRCUIT MODELING METHOD FOR ULTRA-WIDEBAND ANTENNAS

Y. Wang and J. Z. Li

Department of Information and Electronic Engineering
Zhejiang University
Hangzhou 310027, China

L. X. Ran

The Electromagnetics Academy at Zhejiang University
Zhejiang University
Hangzhou 310058, China

Abstract—This paper presents an effective modeling methodology for Ultra-wideband (UWB) antennas. The methodology is based on augmenting an existing narrow-band model with a macro-model while simultaneously perturbing component values of the narrow-band model. The narrow-band model is an empirical-based circuit and the macro-model described by rational functions is determined using data fitting approaches. The perturbation of component values of the narrow-band model is achieved by adjustments in SPICE. This method is demonstrated on the example of a 2.5 cm dipole antenna and a circular disc monopole antenna for UWB systems. Simulation results show that this methodology is effective over a wide bandwidth and suitable for modeling most UWB antennas.

1. INTRODUCTION

Worldwide interest in Ultra-wideband (UWB) [1, 2] wireless has increased greatly with the release in Feb. 2002 by the FCC of their first authorization for UWB in several frequency bands (0–960 MHz, 3.1–10.6 GHz, and 22–29 GHz) [3]. Although the large bandwidth enables short-range, high data-rate communication and high resolution positioning [4], it imposes new design challenges in UWB systems [23, 24]. One challenge is the co-design of UWB antenna/circuit interface. It is necessary to do co-simulation of the antennas with the

UWB transmitter and receiver. Since circuit simulation is traditionally done in a time-domain simulator such as SPICE, a general equivalent circuit model of UWB antennas is required.

There are two basic requirements for the equivalent circuit model of UWB antennas. First, input impedances or admittances of the equivalent circuit model should match up with those of the modeled antenna [5]. In traditional narrowband systems, all the design parameters of antenna are expressed in single values and antennas are modeled as resistors with a standard value. However, the parameters are frequency-dependent in UWB systems, so it is not reasonable using traditional model. Second, load resistor is an important parameter to describe radiated waveforms [6]. In a UWB communication system, the antennas act as major pulse-shaping filters. Bandwidth limitations of the antennas show up as a frequency-domain transfer function and as time-domain distortion of the received pulse [7]. The equivalent circuit model should capture the waveform distortion so that one can compensate at the transmitter/receiver.

Extensive studies have been reported in the literature regarding the determination of the input impedance or admittance function. These include Hamid's graphical fitting method [8], Long's transmission line method [9], Gerrits's intuitive electrical schematic [10], Rambabu's broadband equivalent circuit consisting of a series resonant circuit and two parallel resonant circuits [11], Nie's accurate numerical modeling [12] and Tang's four-element lumped-parameter equivalent circuit [13]. These models above are physically based and propose several equivalent circuit topologies from the aspect of input impedance or admittance matching. A more effective model is the degenerated Foster canonical forms proposed by Wang [14]. The model introduces a load resistor to reproduce the radiated waveform. The resulting impedances match well up to 5 GHz, almost twice the first resonant frequency. There are also studies of antenna modeling regarding field distribution and reflection coefficient. These include Sijher's Genetic Algorithm (GA) optimization method [15], Gustafsson's resonance model [16], Marrocco's approximate space-time-frequency field representation [17], and Shen's modal-expansion method [18].

This paper describes an effective modeling methodology for UWB antennas, the circuit refinement method. First, a narrow-band model as degenerated Foster canonical form is built. Second, the narrow-band model is augmented with a macro-model described by rational functions, and then the macro-model is converted into the equivalent circuits. Finally, the macro-model affects the poles of initial narrow-band model, so perturbation of component values of the narrow-band model is needed. The ultimate model matches the admittances of the

modeled antenna over a wide bandwidth, and reproduces the far-zone E field using the load resistor R_{rad} of the narrow-band model.

This paper is organized as follows. Section 2 presents the concept of circuit refinement method and the details of the modeling method. In Section 3, several practical examples are presented to verify the proposed modeling method.

2. CIRCUIT REFINEMENT METHOD

The initial concept of the circuit refinement method for UWB antennas is introduced in Fig. 1. By fitting admittance data of the antenna obtained by simulation, the antenna is modeled by a narrow-band model augmented with a macro-model. The narrow-band model is an empirical-based circuit and forms the base of the ultimate model. The macro-model described by rational functions is parallel with the narrow-band model and is used to increase the accuracy of input admittance matching. The load resistor R_{rad} reproduces the far-zone E field. The ultimate model preserves the physical intuition of equivalent circuits and utilizes the accuracy of macro-model data fitting.

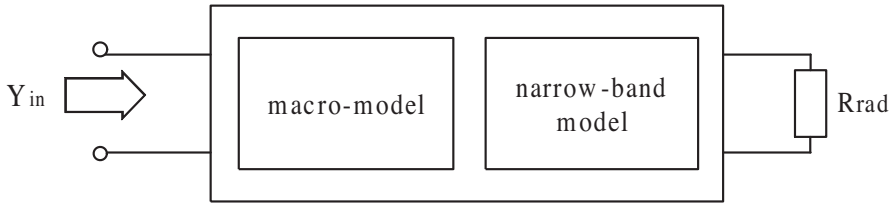

Figure 1. Concept of circuit refinement method.

2.1. Narrow-band Model

Generally, UWB antennas act as band-pass filters, so the circuit topology shown in Fig. 2 is chosen as the narrow-band model. The series resonant circuit C_1, L_1 works as a high-pass filter, while parallel resonant circuit C_2, L_2 as a low-pass filter. The whole circuit works as a band-pass filter and models the UWB antenna roughly. R_{rad} is an important parameter to reproduce the radiated waveform, furthermore, the transfer function. The component values of the narrow-band model can be calculated by utilizing the application bandwidths, center frequencies or resonant frequencies of antennas. The circuit topology has been successfully employed to model the dipole antenna [8].

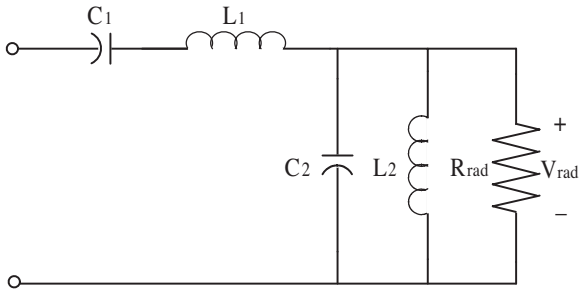

Figure 2. Circuit topology of narrow-band model.

2.2. Macro-model

The narrow-band model serves only as an approximation for the modeling of UWB antennas. The antenna's admittance data obtained from XFDTD is then compared with input admittance of narrow-band model derived in SPICE, and the differences between them are modeled by a macro-model. It is effective to augment the macro-model to guarantee the accuracy of input admittance matching over a wide bandwidth.

Based on the parallel topology, it is straightforward to calculate the macro-model data. The admittance function for the macro-model, $Y_{macro}(\omega_n)$, can be obtained from the admittance parameters of the antennas, $Y_{ant}(\omega_n)$, and of the narrow-band model, $Y_{narrow}(\omega_n)$, as

$$Y_{macro}(\omega_n) = Y_{ant}(\omega_n) - Y_{narrow}(\omega_n). \tag{1}$$

The admittance function $Y_{macro}(\omega_n)$ can be approximated by rational functions in rational polynomial, pole-zero or pole-residue form, such as

$$Y_{macro}(s) = \sum_{i=1}^{Q} \frac{k_i}{s - p_i} + d + se \tag{2}$$

where $s = jw_n$ are the complex frequency points. The unknown parameters k_i, p_i, d and e in (2) are obtained using data fitting approaches, such as vector fitting [19] or least-squares fitting.

After all of the parameters of admittance function are calculated, it is feasible to convert it into circuits using the equivalent circuit for rational approximation of transfer functions and the component values of circuits are derived from calculation [20]. $Y_{macro}(s)$ can be considered as parallel addition of some branch circuits shown as Fig. 3.

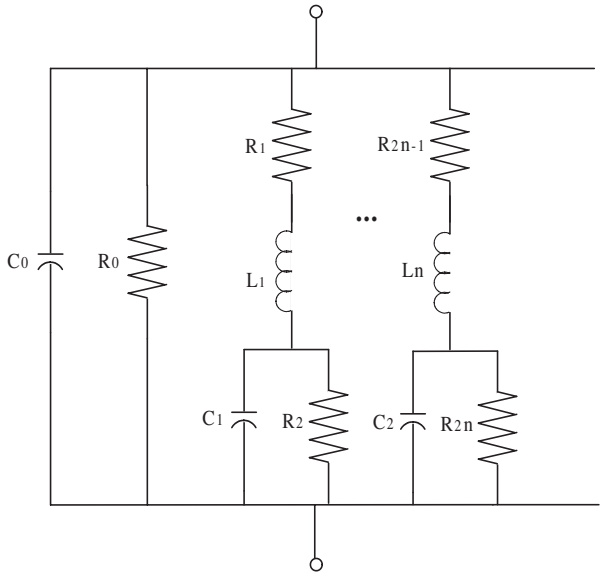

Figure 3. Equivalent circuits of macro-model.

2.3. Perturbation Approach

After the narrow-band model is augmented with the macro-model, the poles of initial narrow-band model have been affected by the augmented macro-model [21], so it is important to modify the component values of narrow-band model to compensate this disadvantage. If the narrow-model is not perturbed, accurate results may require a high-order macro-model network which will increase overall simulation time and be contrary to our philosophy. By appropriately adjust component values of the narrow-band model in SPICE, a relatively lower order macro-model for a given quality of fit can be obtained.

The ultimate model is composed of the perturbed narrow-band model combined with the macro-model. The narrow-band model is shown as Fig. 2 with relevant component values. The macro-model is converted into equivalent circuits shown as Fig. 3. The parallel network of the circuits as Fig. 2 and Fig. 3 composes the ultimate model. From the above, the antennas have been modeled into spice-compatible circuits by circuit refinement method, so it is easy to do the co-simulation of the UWB antennas with the UWB transmitter and receiver in SPICE.

3. EXAMPLE RESULTS

This section demonstrates the application of the circuit refinement method on several antennas, including a dipole antenna and a printed circular disc monopole antenna.

3.1. Modeling a Dipole Antenna

First a small dipole antenna is used to verify the proposed modeling approach. The application bandwidth is from 3.1 to 10.6 GHz, and the center frequency is 6 GHz. The length of dipole antenna is 2.5 cm by calculation.

The circuit shown in Fig. 2 is used as the narrow-band model. The initial component values of narrow-band model are calculated and chosen by $\omega_0^2 = 1/LC$, where ω_0 is the resonant frequency. The optimizations of the component values are made in SPICE so that the input admittance of a narrow-band model should equal to that of the dipole antenna at the center frequency, the component values of narrow-band model can be obtained as $C_1 = 0.12$ pF, $L_1 = 10$ nH, $C_2 = 0.12$ pF, $L_2 = 60$ nH, and R_{rad}= 68 Ω. The resulting admittances from SPICE and XFDTD in Fig. 4 show that the narrow-band model serves only as an approximation to the dipole antenna in input admittance matching from 3.1 GHz to 10.6 GHz.

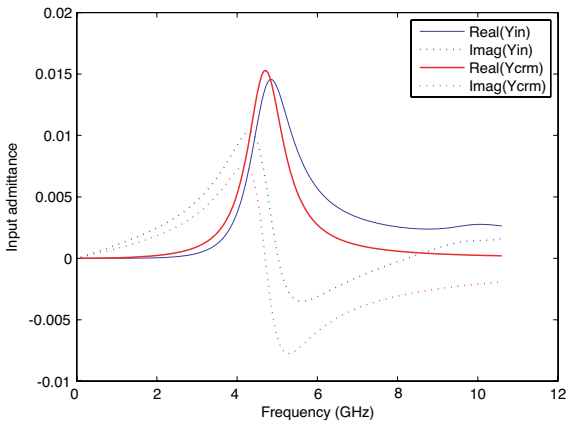

Figure 4. Comparison of admittances of the dipole antenna (Y_{in}) and the narrow-band model (Y_{narrow}).

Then a parallel macro-model is added to refine the narrow-band model. A two-order circuit network is needed by calculation and the

circuit topology as Fig. 3 with two branches is served as the macro-model. The component values of the macro-model are calculated by the method proposed in Section 2.2.

Next, perturbation is applied to the component values of initial narrow-band model. By slightly adjusting the known component values of the narrow-band model in SPICE to achieve a better fitting of input admittance, the component values of the narrow-band model after perturbation are obtained. Table 1 shows the values of the five elements of the narrow-band model before and after perturbation. Fig. 5 compares the admittance of the dipole antenna with that of the ultimate model obtained by circuit refinement method. The admittance of the ultimate model is virtually indistinguishable with that of the dipole antenna.

Table 1. Component values of the narrow-band model before and after perturbation.

	C_1	L_1	C_2	L_2	R_{rad}
Before perturbation	0.12 pF	10 nH	0.12 pF	60 nH	68 Ω
After perturbation	0.118 pF	10.15 nH	0.123 pF	62 nH	69.1 Ω

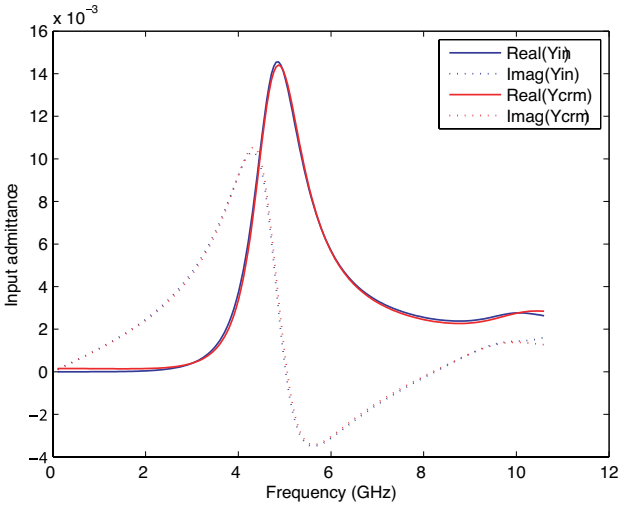

Figure 5. Comparison of admittances of the dipole antenna (Y_{in}) and the ultimate model obtained by circuit refinement method (Y_{crm}).

Finally, the radiated waveform across the load resistor R_{rad} is verified by simulation. A 0.3-ns-wide Gaussian voltage waveform [Fig. 6] is sent into the antenna and the ultimate model. The voltage waveform V_{rad} across the load resistor and the far-zone E field at $\theta = 90^\circ$ at 1 m away from the antenna are derived in SPICE and XFDTD, respectively. Fig. 6 shows that the two normalized waveforms match well after scaling and time shifting, which means the load resistor models the scattered waveform E field perfectly. The ratio of V_{rad} to E_{rad} at 1 m before normalization is approximately 2, so waveform dispersion can be compensated at the transmitter/receiver.

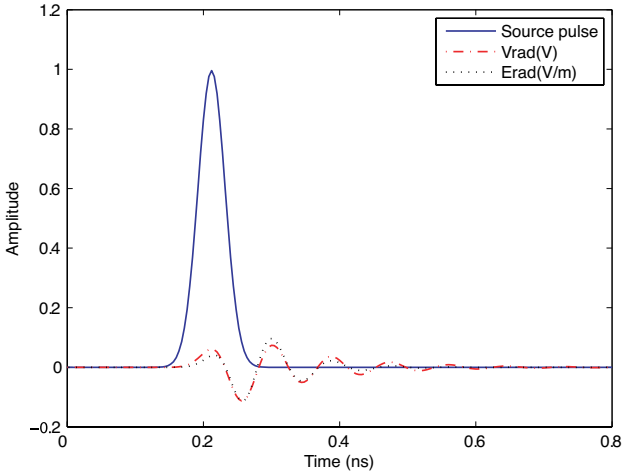

Figure 6. Time-domain waveforms of Gaussian source pulse with a width of 0.3 ns, normalized V_{rad} form SPICE and E_{rad}(in $\theta = 90^\circ$) from XFDTD.

3.2. Modeling a Printed Circular Disc Monopole Antenna

A printed circular disc monopole antenna, shown in Fig. 7, has been proposed as a typical UWB antenna [22]. The circuit shown in Fig. 2 is used as the narrow-band model. The initial component values of narrow-band model are calculated and chosen by $\omega_0^2 = 1/LC$, where ω_0 is the resonant frequency. The optimizations of the component values are made in SPICE so that the input admittance of a narrow-band model should equal to that of the printed circular disc monopole antenna at the center frequency, the component values can be obtained as C_1= 0.12 pF, L_1 = 10.2 nH, C_2 = 0.1 pF, L_2 = 3.5 nH, and R_{rad} = 27.8 Ω. The resulting admittances from SPICE and XFDTD in

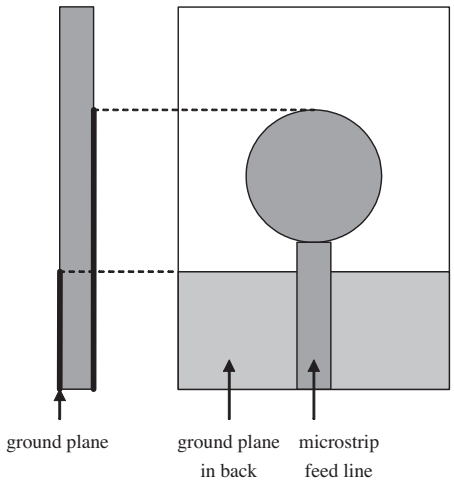

Figure 7. A printed circular disc monopole antenna.

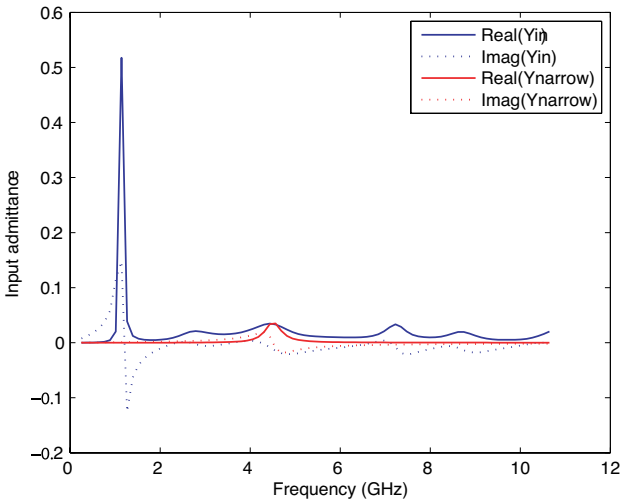

Figure 8. Comparison of admittances of the monopole antenna (Y_{in}) and the narrow-band model (Y_{narrow}).

Fig. 8 show that the narrow-band model only works well in a narrow bandwidth.

Then a parallel macro-model is added to refine the narrow-band model. A six-order circuit network is needed by calculation and the

Table 2. Component values of the narrow-band model before and after perturbation.

	C_1	L_1	C_2	L_2	R_{rad}
Before perturbation	0.12 pF	10.2 nH	0.1 pF	3.5 nH	27.8 Ω
After perturbation	0.118 pF	10.18 nH	0.11 pF	3.6 nH	27.7 Ω

circuit topology as Fig. 3 with six branches is served as the macro-model. The component values of the macro-model are calculated by the method proposed in Section 2.2.

Finally, perturbation is applied to the parameters of initial narrow-band model during the circuit refinement process. By slightly adjusting the known component values of the narrow-band model in SPICE to achieve a better fitting of input admittance, the component values of the narrow-band model after perturbation are obtained. Table 2 shows the values of the five elements of the narrow-band model before and after perturbation. Fig. 9 compares the admittance of the monopole antenna with that of the ultimate model obtained by circuit refinement method. The admittance of the ultimate model is virtually indistinguishable with that of the monopole antenna.

From the above it is shown that the circuit refinement method works effectively over a large bandwidth and is suitable for modeling of UWB antennas.

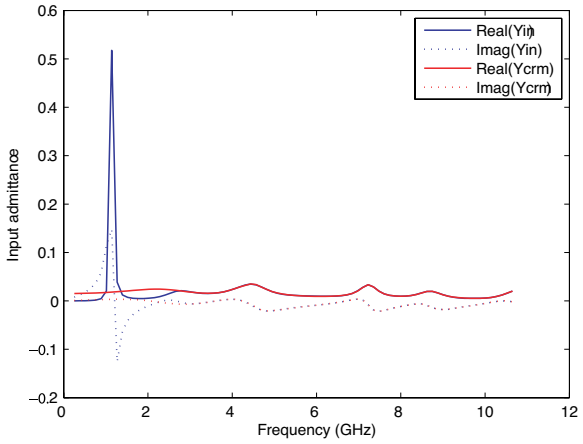

Figure 9. Comparison of admittances of the monopole antenna (Y_{in}) and the ultimate model obtained by circuit refinement method (Y_{crm}).

4. CONCLUSION

An equivalent circuit modeling method has been presented for the broadband circuit models of UWB antennas that are compatible with time-domain circuit simulators. The main philosophy is to take advantage of the physical information provided by an existing narrow-band model and use data fitting approach to automatically develop a suitable macro-model which improves the overall performance of the ultimate model.

One of the key advantages of the hybrid narrow-band model with a macro-model compared to complete macro-model is the reduced complexity of the circuits describing the macro-model network, which generally improves the robustness of the data fitting process. Perturbation of component values of the narrow-band model is used to guarantee the accuracy of modeling. The ultimate model works well as far as 10.6 GHz, theoretically to more, and takes into account the waveform dispersion, which is useful for compensation at transmitter/receiver. The new methodology should be useful for modeling a wide range of UWB antennas.

ACKNOWLEDGMENT

The work is sponsored by the Zhejiang Natural Science Foundation (ZJNSF) under grants No. Y106360 and No. R105253, the NSFC (Nos. 60531020, 60671003), the NCET-07-0750, and the Ph.D. Programs Foundation of MEC (No. 20070335120).

REFERENCES

1. Chen, F. C. and W. C. Chew, "Time-domain ultra-wideband microwave imaging radar system," *Journal of Electromagnetic Waves and Applications*, Vol. 17, 313–331, 2003.
2. Fan, Z., L. X. Ran, and J. A. Kong, "Source pulse optimizations for UWB radio systems," *Journal of Electromagnetic Waves and Applications*, Vol. 20, 1535–1550, 2006.
3. "Revision of Part 15 of the Commission's rules regarding ultra-wideband transmission systems," FCC Notice of Proposed Rule Making, ET-Docket 98-153.
4. Liu, X., B.-Z. Wang, S. Xiao, and J. Deng, "Performance of impulse radio UWB communications based on time reversal technique," *Progress In Electromagnetics Research*, PIER 79, 401–413, 2008.

5. Liu, S. F., X. W. Shi, and S. D. Liu, "Study on the impedance-matching technique for high-temperature superconducting microstrip antennas," *Progress In Electromagnetics Research*, PIER 77, 281–284, 2007.
6. Uduwawala, D., "Modeling and investigation of planar parabolic dipoles for GPR applications: A comparison with bow-tie using FDTD," *Journal of Electromagnetic Waves and Applications*, Vol. 20, 227–236, 2006.
7. Akhoondzadeh-Asl, L., M. Fardis, A. Abolghasemi, and G. Dadashzadeh, "Frequency and time domain characteristic of a novel notch frequency UWB antenna," *Progress In Electromagnetics Research*, PIER 80, 337–348, 2008.
8. Hamid, M. and R. Hamid, "Equivalent circuit of dipole antenna of arbitrary length," *IEEE Trans. Antennas Propag.*, Vol. 45, No. 11, 1695–1696, Nov. 1997.
9. Long, B., P. Werner, and D. Werner, "A simple broadband dipole equivalent circuit model," *IEEE APS Int. Symp. Dig.*, Vol. 2, 1046–1049, Slat Lake City, USA, Jul. 2000.
10. Gerrits, J., A. Hutter, J. Ayadi, and J. Farserotu, "Equivalent circuit of dipole antenna of arbitrary length," *Proceedings of the 2003 International Workshop on Ultra Wideband Systems*, Vol. 1, Oulu, Finland, June 2–5, 2003.
11. Rambabu, K., M. Ramesh, and A. T. Kalghatgi, "Broadband equivalent circuit of a dipole antenna," *IEE Proc. - Microw. Antennas Propag.*, Vol. 41, 100–103, Jan. 1993.
12. Nie, X. C., N. Yuan, L. W. Li, and Y. B. Gan, "Accurate modeling of monopole antennas in shielded enclosures with apertures," *Progress In Electromagnetics Research*, PIER 79, 251–262, 2008.
13. Tang, T. G., Q. M. Tieng, and M. W. Gunn, "Equivalent circuit of a dipole antenna using frequency-independent lumped elements," *IEEE Trans. Antennas Propag.*, Vol. 146, No. 3, 391–393, Dec. 1999.
14. Wang, S., A. Niknejad, and R. Brodersen, "Circuit modeling methodology for UWB omnidirectional small antennas," *IEEE Journal on Selected Areas in Communications*, Vol. 24, No. 4, 871–877, Apr. 2006.
15. Sijher, T. S. and A. A. Kishk, "Antenna modeling by infinitesimal dipoles using genetic algorithms," *Progress In Electromagnetics Research*, PIER 52, 225–254, 2005.

16. Gustafsson, M. and S. Nordebo, "Bandwidth, Q factor, and resonance models of antennas," *Progress In Electromagnetics Research*, PIER 62, 1–20, 2006.
17. Marrocco, G., M. Migliorelli, and M. Ciattaglia, "Simultaneous time-frequency modeling of ultra-wideband antennas by two-dimensional hermite processing," *Progress In Electromagnetics Research*, PIER 68, 317–337, 2007.
18. Shen Z. and R. H. MacPhie, "Theoretical Modeling of Multi-Sleeve Monopole Antennas," *Progress In Electromagnetics Research*, PIER 31, 31–54, 2001.
19. Gustavsen, B. and A. Semlyen, "Rational approximation of frequency domain responses by vector fitting," *IEEE Trans. Power Del.*, Vol. 14, No. 3, 1052–1061, Jul. 1999.
20. Antonini, G., "Spice equivalent circuits of frequency-domain responses," *IEEE Trans. Electromagnetic Compatibility*, Vol. 45, No. 3, 502–512, Aug. 2003.
21. Kolstad, J., C. Blevins, J. Dunn, and A. Weisshaar, "A new circuit augmentation method for modeling of interconnects and passive components," *IEEE Trans. Advanced Packaging*, Vol. 20, No. 1, 67–77, Feb. 2006.
22. Liang, J., C. Chiau, X. Chen, and C. Parini, "Study of a printed circular disc monopole antenna for UWB systems," *IEEE Trans. Antennas Propag.*, Vol. 53, No. 11, 3500–3504, Nov. 2005.
23. Joardar, S. and A. B. Bhattacharya, "A novel method for testing ultra wideband antenna-feeds on radio telescope dish antennas," *Progress In Electromagnetics Research*, PIER 81, 41–59, 2008.
24. Joardar, S., M. Jaint, V. Bandewar, and A. B. Bhattacharya, "An innovative portable ultra wide band stereophonic radio direction finder," *Progress In Electromagnetics Research*, PIER 78, 255–264, 2008.